Transverse instabilities in the polarizations and intensities of counterpropagating light waves

Alexander L. Gaeta* and Robert W. Boyd
Institute of Optics, University of Rochester, Rochester, New York 14627
(Received 1 March 1993)

We present a theoretical analysis of the stability characteristics of each of the four eigenpolarization configurations of two light waves counterpropagating through a nonlinear medium. Our treatment generalizes previous treatments in that we allow the possibility of the development of transverse instabilities in either the intensities or the polarizations of the waves. Indeed, we find that under many conditions the instability develops in directions other than the symmetry axis of the interaction and that the instability can affect the intensity or the polarization of the waves. We also find through numerical computations that the polarizations of the waves can become unstable in the nonlinear regime at intensities above the threshold for the transverse amplitude instability but below the threshold predicted by linear stability analysis for the corresponding polarization instability. We conclude that in many cases the inclusion of the tensor properties of the nonlinear interaction is important in describing the dynamical behavior of counterpropagating waves.

PACS number(s): 42.65.Vh

The situation of two light waves counterpropagating through a nonlinear medium is of interest because such a configuration is present in many optical devices, such as certain phase conjugate mirrors and optical switches. Any instabilities that could occur in the propagation of such light waves would be expected to affect adversely the performance of the optical device. From a different perspective, the behavior of two counterpropagating light waves is of interest at a conceptual level, because this apparently simple situation can lead to very complicated behavior such as bistability and to instabilities including chaos. One reason why the interaction of counterpropagating light waves leads to such rich behavior is that the interaction displays aspects of nonlocality and time delay, even for the case (assumed within this paper) in which the nonlinear responses of the material system is both local and instantaneous. The origin of this behavior is that, for example, the instantaneous value of the intensity of the backward-going wave at some representative point in the material can influence the propagation of the forward-going wave as it passes this point. This portion of the forward-going wave can subsequently influence the propagation of that portion of the backward-going wave that has not yet reached the initial point, and in this manner the backward-going wave can influence its own propagation in a nonlocal and time-delayed fashion. At a mathematical level, this behavior results from the fact that the propagation of the forward- and backward-going waves are described by partial differential equations, and (unlike in the case of a single forward-going wave) these equations cannot be transformed trivially into an ordinary differential equation by introducing the local time $t-z/v$ (where v is the velocity of light in the material medium). Similarly, the boundary conditions for the problem must be specified at two different locations for the forward- and backward-going waves. As a consequence of these mathematical properties, counterpropagating light waves can give rise both to convective instabilities (i.e., to instabilities that grow in space) and to absolute instabilities (i.e., to instabilities that grow in time and lead possibly to temporal chaos), whereas a single light wave can give rise only to convective instabilities.

REVIEW OF PREVIOUS WORK ON INSTABILITIES OF COUNTERPROPAGATING WAVES

One of the early studies of the stability characteristics of counterpropagating waves was that of Silberberg and Bar-Joseph [1,2]. Their treatment described the interacting waves in the scalar approximation, they found that the waves could become unstable, but only for a nonlinear medium with noninstantaneous response. The instability could lead either to periodic or to chaotic fluctuations. They ascribed the origin of this instability to a gain-feedback mechanism in which gain is present (as in stimulated Rayleigh-wing scattering) at frequency sidebands of the incident waves detuned by approximately the inverse of the medium response time and in which feedback is present because these sidebands can scatter from the grating established in the medium by the interference of the two incident waves. More recently [3] this model has bene extended to apply to the situation in which the nonlinear response is provided by a collection of two-level atoms, a situation in which instabilities have been observed experimentally [4]. In addition, it has recently been shown by Law and Kaplan [5] that instabilities can occur as the result of the combined action of optical nonlinearity and linear dispersion.

The importance of polarization effects in determining the stability characteristics of counterpropagating waves in an isotropic nonlinear medium has been established from several different considerations [6]. In 1978, Pepper, Fekete, and Yariv [7] observed amplified reflection and parametric oscillation in a collinear four-wave-mixing interaction in which the pump and signal waves were orthogonally polarized. These results were interpreted in terms of a theoretical model [8] of the phase-conjugation process, but in fact also provide a demonstration of a polarization instability of counterpropagating light waves. In 1980, Winful and Marburger [9] showed that hysteresis and optical bistability can occur in the process of degenerate four-wave mixing in the geometry used to produce phase conjugation. This sort of analysis was later extended by Lytel [10] and by Kaplan and Law [11] to show that hysteresis and bistability could occur in the polarizations of interacting waves in a strictly collinear geometry. These predictions were subsequently verified experimentally by Gauthier *et al.* [12].

In 1983, Kaplan [13] showed that counterpropagating optical waves possess four eigenpolarizations, namely the arrangements in which the polarizations of the counterpropagating waves are linear and parallel, linear and perpendicular, circular and corotating, and circular and counterrotating. If the input waves have polarizations other than one of these eigenarrangements, the polarization of each wave will vary with position within the nonlinear medium. Mathematically, the eigenpolarizations possess the property that the propagation equations [see Eqs. (4) below] possess steady-state solutions for which the polarization of each wave is spatially invariant. The original analysis of Kaplan did not address whether these eigenpolarizations were stable or unstable to the growth of small perturbations. However, in 1986 Wabnitz and Gregori [14] performed a linear stability analysis of the spatial dependence of these solutions for the case of a medium with instantaneous response and showed that two of these eigenpolarizations, namely linear parallel and circular corotating, were always stable whereas the other two eigenpolarizations, linear perpendicular and circular counterrotating, could become unstable for certain ratios of the input intensities for materials with certain tensor properties [in particular, for certain values of the ratio B/A in the notation of Eq. (4) below]. Tratnik and Sipe [15] showed that for an isotropic medium these spatial instabilities could not lead to chaos, although spatially chaotic behavior could occur for propagation along certain types of symmetry axes in anisotropic materials, as had been pointed out earlier for one particular case by Yumoto and Otsuka [16]. One should note that the spatial instabilities analyzed in Refs. [14]–[16] are convective instabilities and correspond physically to the situation in which the polarizations of the input beams do not correspond exactly to an eigenpolarization. The solutions are unstable in the sense that the deviation of the input polarization from the input polarization becomes more pronounced with propagation distance through the nonlinear medium.

In 1987, Gaeta *et al.* [17] studied the temporal stability of the eigenpolarizations of counterpropagating waves and found that the configuration of linear and parallel input polarizations, which as mentioned above is spatially stable, nonetheless can become unstable to the growth of temporal fluctuations. Under certain conditions involving high input intensities, these fluctuations were shown to be chaotic in nature. (The case of circular and corotating input polarizations was found to be stable to temporal as well as spatial fluctuations for a medium with instantaneous response, a result that might be expected on the basis of angular momentum conservation.) These predictions were subsequently verified experimentally by Gauthier, Malcuit, and Boyd [18].

The instabilities mentioned above (except for those of Refs. [7] and [8]) are instabilities that occur on the system axis and can be described theoretically by a one-dimensional theory. Under certain conditions, instabilities are predicted [19,20] to develop in the transverse structure of the interacting waves, and in fact such transverse instabilities have been observed experimentally [12,21]. A prime example is self-oscillation in the process of phase conjugation (i.e., infinite phase-conjugate reflectivity) by degenerate four-wave mixing, a possibility that was pointed out as early as 1977 by Yariv and Pepper [8]. In the notation of Ref. [8], the phase-conjugate intensity reflectivity is given by $R=\tan^2|\kappa|L$, where L is the interaction path length and κ is the nonlinear coupling constant proportional to $\chi^{(3)}$ times the product of pump wave amplitudes. For $|\kappa|L=\pi/2$, the reflectivity becomes formally infinite, indicating that off-axis waves will be spontaneously generated by the four-wave-mixing process. However, for directions near the axis defined by the pump waves, nonlinear optical processes not included in the analysis of Yariv and Pepper such as forward four-wave mixing can become phase matched as a result of the nonlinear contribution to the wave vector of the interacting waves, and the presence of such processes can modify the threshold for instability.

Under certain circumstances off-axis instabilities can develop having complex transverse spatial patterns, including rings [18,22,23], emission of a pattern with fourfold symmetry [18,24] and with sixfold symmetry (hexagons) [23]. Detailed studies have been performed to determine the conditions under which various types of transverse patterns can occur [24]. Grynberg has pointed out that the tendency for hexagons to be formed can be understood from the point of view that phase-matched near-forward four-wave-mixing processes can lead to mutual reinforcement of a pattern with sixfold symmetry [25]. Moreover, Chang *et al.* [26] have performed numerical calculations of the interaction of counterpropagating waves that predict the generation of hexagonal patterns.

THEORETICAL GROUNDWORK

We assume that the fields inside the nonlinear medium propagate nearly parallel to the z axis such that the fields are polarized in a plane parallel to the x-y plane. The total complex electric field $\mathbf{E}(\mathbf{r},t)$ centered at a frequency ω inside the nonlinear medium can then be expressed as

$$\mathbf{E}(\mathbf{r},t)=\sum_j [E_j(\mathbf{r},t)\hat{\mathbf{u}}_j]e^{-i\omega t}\,, \tag{1}$$

where $\hat{\mathbf{u}}_j$ is the unit vector for the particular polarization basis that is being used and E_j is the amplitude of the $\hat{\mathbf{u}}_j$-polarized field. For example, in the Cartesian basis, $j=x,y$ and $\hat{\mathbf{u}}_x=\hat{\mathbf{x}}$ and $\hat{\mathbf{u}}_y=\hat{\mathbf{y}}$, and in the circularly polarized basis, $j=+,-$ and $\hat{\mathbf{u}}_\pm=(\hat{\mathbf{x}}\pm i\hat{\mathbf{y}})/\sqrt{2}$. Similarly, we assume that the nonlinear polarization is given by

$$\mathbf{P}(\mathbf{r},t)=\sum_j [P_j(\mathbf{r},t)\hat{\mathbf{u}}_j]e^{-i\omega t} , \tag{2}$$

where P_j is the amplitude of the polarization in the $\hat{\mathbf{u}}_j$ direction. We can express the components of the nonlinear polarization in terms of a field-dependent susceptibility tensor χ_{ij} such that

$$P_i=\sum_{j=x,y}\chi_{ij}E_j . \tag{3}$$

Thus χ_{ij} represents the nonlinear coupling of the jth component of the field to the ith component. The form of χ_{ij} for an isotropic Kerr medium in the linearly polarized and circularly polarized bases will be introduced below.

We next assume that the total field inside the medium is composed of forward-traveling and backward-traveling fields with wave-vector amplitudes given by $k=n\omega/c$ where n is the linear index of refraction of the medium. In this case, the following equations for the forward- and backward-traveling field components can be derived from the driven wave equation and Eqs. (1)–(3),

$$\left[\frac{\partial}{\partial z}+\frac{n}{c}\frac{\partial}{\partial t}-i\frac{\nabla_\perp^2}{2k}\right]F_i=i\frac{2\pi\omega}{nc}\sum_j[\chi_{ij}^{(0)}F_j+\chi_{ij}^{(2k)}B_j] \tag{4a}$$

and

$$\left[-\frac{\partial}{\partial z}+\frac{n}{c}\frac{\partial}{\partial t}-i\frac{\nabla_\perp^2}{2k}\right]B_i=i\frac{2\pi\omega}{nc}\sum_j[\chi_{ij}^{(0)}B_j+\chi_{ij}^{(-2k)}F_j] , \tag{4b}$$

where $\nabla_\perp^2$ is the transverse Laplacian, $\chi_{ij}^{(0)}$ and $\chi_{ij}^{(\pm 2k)}$ are the dc and $\pm 2k$ spatial Fourier components of χ_{ij}, respectively, and F_i and B_i are the amplitudes of the ith component of the forward- and backward-traveling waves, respectively. Equations (4) form the basis for our study of instabilities of counterpropagating fields in a nonlinear medium.

The following section gives the results of a temporal stability analysis of the amplitudes and the polarizations of the steady-state solutions to Eqs. (4) for the four eigenpolarization configurations. In the stability analysis, we seek solutions that grow exponentially in time [i.e., $\exp(\lambda t)$] such that $\text{Re}(\lambda)>0$. We then plot the boundary of instability which corresponds to $\text{Re}(\lambda)=0$. For all the cases that we discuss here, we assume that the input intensities of the forward- and backward-traveling waves are equal. This assumption leads to the prediction of only nonoscillatory instabilities $\text{Im}(\lambda)=0$ for the system at threshold [i.e., $\text{Re}(\lambda)=0$]. If the input intensities are unequal, oscillatory instabilities [i.e., $\text{Im}(\lambda)\neq 0$] can occur [27]. However, as the parameter space is large even for equal input intensities, we have decided that consideration of these effects is beyond the scope of the present paper and that these results should be considered in a future publication.

STABILITY ANALYSIS OF EIGENPOLARIZATION CONFIGURATIONS

We first consider the temporal stability of the linearly polarized eigenpolarizations. In the linearly polarized basis, the field-dependent susceptibility for an isotropic lossless nonlinear medium is given by

$$\chi_{ij}=\left[A-\frac{B}{2}\right]\mathbf{E}\cdot\mathbf{E}^*\delta_{ij}+\frac{B}{2}(E_iE_j^*+E_i^*E_j) , \tag{5}$$

where A and B are the real nonlinear coefficients that describe the tensor Kerr nonlinearity for the isotropic medium. For example, for the case of the Kerr effect that results respectively from molecular orientation, from a nonresonant electronic nonlinearity, and from electrostriction, the ratio of the two coefficients is given by $B/A=6$, 1, and 0. The expression for χ_{ij} in Eq. (5) assumes that the response time of the medium is much shorter than the transit time of light through the medium.

For the case of the linear and parallel eigenpolarization, we assume that the input fields are polarized along the x direction, in which case the steady-state solution for the field amplitudes is given by

$$F_x^{SS}(z)=\sqrt{I_f}\exp[ik(A'+B'/2)(I_f+2I_b)z] , \tag{6a}$$

$$B_x^{SS}(z)=\sqrt{I_b}\exp[-ik(A'+B'/2)(2I_f+I_b)z] , \tag{6b}$$

$$B_y^{SS}(z)=0 , \tag{6c}$$

$$F_y^{SS}(z)=0 , \tag{6d}$$

where $A'=4\pi^2A/n^3c^2$ and $B'=4\pi^2B/n^3c^2$ are the renormalized nonlinear coefficients and $I_f=(nc/2\pi)|F_x^{SS}(0)|^2$ and $I_b=(nc/2\pi)|B_x^{SS}(L)|^2$ are the input intensities of the forward and backward waves, respectively. The forward and backward waves remain polarized along the x direction and each x component simply experiences a nonlinear phase shift. In order to determine the temporal stability of the steady-state solutions (6), we perform a linear stability analysis of both the amplitude and the polarization of the total field inside the medium by assuming that

$$\begin{aligned}\mathbf{E}(\mathbf{r},t)=&\{[F_x^{SS}(z)+\delta F_x(\mathbf{r}_\perp,z,t)]\hat{\mathbf{x}}\\&+\delta F_y(\mathbf{r}_\perp,z,t)\hat{\mathbf{y}}\}e^{i(kz-\omega t)}\\&+\{[B_x^{SS}(z)+\delta B_x(\mathbf{r}_\perp,z,t)]\hat{\mathbf{x}}\\&+\delta B_y(\mathbf{r}_\perp,z,t)\hat{\mathbf{y}}\}e^{i(-kz-\omega t)}\end{aligned} \tag{7}$$

where δF_x (δB_x) and δF_y (δB_y) represent the forward- (backward-) traveling perturbation fields polarized along the x and y directions, respectively. The details of the analysis are presented in part 1 of the Appendix. We allow the perturbations to grow off axis so that the transverse stability of the amplitude and of the polarization of this eigenpolarization configuration can also be explored.

Figure 1 shows the results of the stability analysis in which we plot the normalized threshold intensity

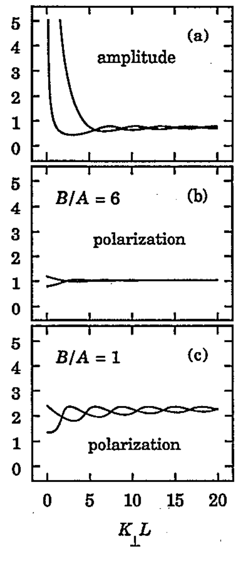

FIG. 1. Normalized threshold intensity P for the linear and parallel eigenpolarization configuration plotted as a function of the transverse wave-vector parameter $K_\perp L$ for (a) the amplitude instability for any value of B/A and for the polarization instability for (b) $B/A=6$ and (c) $B/A=1$. Equal input intensities for the forward- and backward-traveling waves are assumed.

$P=k(A'+B'/2)IL$ for instability as a function of the normalized transverse wave vector $K_\perp L=(k_x^2+k_y^2)L/2k$ for the perturbation for the case in which the input intensities are equal ($I_f=I_f=I$). This normalization for the intensity is used since, for a linearly polarized wave, P represents the nonlinear phase shift in radians imparted by the field on itself. In the limit of large $K_\perp L$, we expect that the results for the threshold intensity should approach the value P_∞ predicted for phase-conjugate oscillation for the corresponding field amplitudes. For all the cases treated in this paper, the value of P_∞ can be easily calculated from the equations for the perturbing field amplitudes given in the Appendix. For example, for the perturbing field amplitudes that are polarized parallel to the linear and parallel eigenpolarization, the value of P_∞ is determined by setting the absolute value of the term (i.e., $|i2\sqrt{P_fP_b}|=2P$) in Eq. (A6) which couples the forward Stokes perturbation field $f_x^{S'}$ to the backward anti-Stokes perturbation field $b_x^{a'*}$ equal to $\pi/2$. This term is equivalent to the coupling constant κ from the four-wave mixing-theory of Yariv and Pepper [8].

Figure 1(a) shows the well-known result [19] for the transverse amplitude instability for scalar waves, which does not depend on the ratio of B/A. In this case, we see that the value of $P\approx 0.45$ for the threshold intensity at $K_\perp L\approx 3$ is considerably lower than the threshold of $P_\infty=\pi/4$. The results for the polarization instability depend on the value of B/A, and in Figs. 1(b) and 1(c) the threshold intensity P for $B/A=6$ and $B/A=1$ are shown. The results in Fig. 1(b) are the same as previously calculated [28]. For the case $B/A=0$, the threshold intensity for the polarization instability is found to be infinite for all values $K_\perp L$. The threshold for phase-conjugate oscillation for the orthogonally polarized perturbation fields is given by $P_\infty=(2A/B+1)\pi/4$. In both cases shown, the instability threshold of $P\approx 0.8$ for $B/A=6$ and $P\approx 1.2$ for $B/A=1$ is lowest on axis $K_\perp L=0$ and is below P_∞. Nevertheless, since the threshold for the amplitude instability is lower than that for the polarization instability for this eigenpolarization configuration, it is expected that the system will become unstable by means of amplitude fluctuations.

We next consider the case of the linear and perpendicular eigenpolarization. The forward- and backward-traveling input fields are taken to be polarized in the x and y directions, respectively. In this case the steady-state solutions for the field amplitudes are given by

$$F_x^{SS}(z)=\sqrt{I_f}\exp\{ik[(A'+B'/2)I_f+A'I_b]z\}\ , \tag{8a}$$

$$B_y^{SS}(z)=\sqrt{I_b}\exp\{-ik[A'I_f+(A'+B'/2)I_b]z\}\ , \tag{8b}$$

$$F_y^{SS}(z)=0\ , \tag{8c}$$

$$B_x^{SS}(z)=0\ , \tag{8d}$$

where $I_f=(nc/2\pi)|F_x^{SS}(0)|^2$ and $I_b=(nc/2\pi)|B_y^{SS}(L)|^2$ are the input intensities of the forward and backward waves, respectively. As expected in the unperturbed solution, the forward and backward waves in the medium remain polarized along the x and y axes, respectively. We perturb this solution by assuming that the total field inside the medium is given by

$$\begin{aligned}\mathbf{E}(\mathbf{r},t)=&\{[F_x^{SS}(z)+\delta F_x(\mathbf{r}_\perp,z,t)]\hat{\mathbf{x}}\\&+\delta F_y(\mathbf{r}_\perp,z,t)\hat{\mathbf{y}}\}e^{i(kz-\omega t)}\\&+\{\delta B_x(\mathbf{r}_\perp,z,t)\hat{\mathbf{x}}\\&+[B_y^{SS}(z)+\delta B_y(\mathbf{r}_\perp,z,t)]\hat{\mathbf{y}}\}e^{i(-kz-\omega t)}\ .\end{aligned} \tag{9}$$

The details of the linear stability analysis are given in part 2 of the Appendix.

The results of the analysis for the case of equal input intensities are shown in Fig. 2 where we plot the threshold intensity P for the amplitude instability [Figs. 2(a)–2(c)] and the polarization instability [Figs. 2(d)–2(f)] as functions of $K_\perp L$ for various values of B/A. The threshold for the amplitude instability does depend on B/A, which is to be expected since P is proportional to $A+B/2$, whereas the cross phase modulation exhibited in Eqs. (8a) and (8b) depends only on A. The threshold intensity for phase-conjugate oscillation of the perturbing fields polarized parallel to the steady-state input fields is given by $P_\infty=(1+B/2A)\pi/2$ and thus (for values of A and B that are of the same sign) is smallest for $B/A=0$. The minimum values for the threshold intensity for the amplitude instability all occur off axis ($K_\perp L\neq 0$) for $B/A=6$, 1, and 0, and are given by $P\approx 1.8$, 1, and 0.8, respectively, which in all cases are lower than the associated value of P_∞. For the polarization instability, the behavior is more complicated. The threshold for phase-conjugate oscillation is given by $P_\infty=(1+B/2A)\pi/|2-B/A|$. For the case $B/A=6$, the lowest threshold value $P\approx 1.5$ for the polarization instability occurs on axis and is lower than the value of P for the amplitude in-

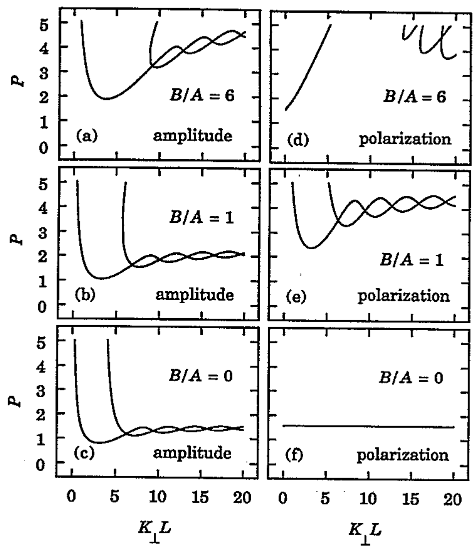

FIG. 2. Normalized threshold intensity P for the linear and perpendicular eigenpolarization configuration plotted as a function of the transverse wave-vector parameter $K_{pd}L$ for (a)–(c) the amplitude instability and for (d)–(f) the polarization instability for (a) and (d) $B/A=6$, (b) and (e) $B/A=1$, and (c) and (f) $B/A=0$. Equal input intensities for the forward- and backward-traveling waves are assumed.

stability. For $B/A=1$, the lowest value $P\approx 2.3$ for instability occurs off axis and is higher than the value than for the corresponding amplitude instability. For $B/A=0$, the threshold $P\approx 1.6$ for instability is independent of $K_\perp L$ and thus is most likely to occur on axis since typically there would be more noise in that direction to initiate the instability. Nevertheless, the minimum threshold value for the polarization instability for $B/A=0$ is larger than the corresponding minimum value for the amplitude instability.

We next investigate the stability properties of the circularly polarized eigenpolarizations. The field components and the nonlinear polarization components are transformed from the linearly polarized basis to the circular polarized basis through use of the following transformations:

$$\begin{bmatrix} E_+ \\ E_- \end{bmatrix} = \underline{M} \begin{bmatrix} E_x \\ E_y \end{bmatrix} , \tag{10a}$$

$$\begin{bmatrix} P_+ \\ P_- \end{bmatrix} = \underline{M} \begin{bmatrix} P_x \\ P_y \end{bmatrix} , \tag{10b}$$

where $\underline{M}$ is the matrix given by

$$\underline{M} = \frac{1}{\sqrt{2}} \begin{bmatrix} 1 & i \\ 1 & -i \end{bmatrix} . \tag{10c}$$

The elements of the field-dependent susceptibility tensor χ_{ij} in the circularly polarized basis are then related to the elements of the field-dependent susceptibility tensor χ_{ij} in the linearly polarized basis by

$$\begin{bmatrix} \chi_{++} & \chi_{+-} \\ \chi_{-+} & \chi_{--} \end{bmatrix} = \underline{M} \begin{bmatrix} \chi_{xx} & \chi_{xy} \\ \chi_{yx} & \chi_{yy} \end{bmatrix} \underline{M}^{-1} . \tag{11}$$

The expressions for χ_{ij} in the circularly polarized basis are thus given by

$$\chi_{++} = \chi_{--} = A(\mathbf{E}\cdot\mathbf{E}^*) , \tag{12a}$$

$$\chi_{+-} = \chi_{-+}^* = BE_+E_-^* . \tag{12b}$$

The expressions (12) for field-dependent susceptibility tensor χ_{ij} ($i=+,-;j=+,-$) are used with Eqs. (4) to describe the propagation of the forward- and backward-traveling circularly polarized components. The forms for $\chi_{\pm\pm}$ and $\chi_{\pm\mp}$ are particularly simple for an isotropic medium because there does not exist a preferred direction, and thus the circular basis forms a more natural basis for the system than the Cartesian basis. The physical meaning of the A and B coefficients is apparent from Eqs. (12). The coefficient A determines the strength of the nonlinear coupling experienced by each circularly polarized component as a result of the total intensity [Eq. (12a)], whereas the coefficient B determines the strength of the coupling between two polarization components of opposite handedness [Eq. (12b)].

We now consider the case of the eigenpolarization configuration in which the two input waves are circular and corotating. The steady-state solutions to Eqs. (4) for the case in which the incident waves are $\hat{\sigma}_+$ polarized are given by

$$F_+^{SS}(z) = \sqrt{I_f}\exp[ikA'(I_f+2I_b)z] , \tag{13a}$$

$$B_+^{SS}(z) = \sqrt{I_b}\exp[-ikA'(2I_f+I_b)z] , \tag{13b}$$

$$F_-^{SS}(z) = 0 , \tag{13c}$$

$$B_-^{SS}(z) = 0 , \tag{13d}$$

where $I_f=(nc/2\pi)|F_+^{SS}(0)|^2$ and $I_b=(nc/2\pi)|B_+^{SS}(L)|^2$ are the input intensities of the forward and backward waves, respectively. The steady-state solutions (13) are similar to the solutions for the linear and parallel polarization except that in the circularly polarized case only the coefficient A determines the magnitude of the phase shift. We perturb the amplitude and polarization of the steady-state fields by assuming that the total field inside the medium is given by

$$\begin{aligned} \mathbf{E}(\mathbf{r},t) = & \{[F_+^{SS}(z)+\delta F_+(\mathbf{r}_\perp,z,t)]\hat{\sigma}_+ \\ & +\delta F_-(\mathbf{r}_\perp,z,t)\hat{\sigma}_-\}e^{i(kz-\omega t)} \\ & +\{[B_+^{SS}(z)+\delta B_+(\mathbf{r}_\perp,z,t)]\hat{\sigma}_+ \\ & +\delta B_-(\mathbf{r}_\perp,z,t)\hat{\sigma}_-\}e^{i(-kz-\omega t)} \end{aligned} \tag{14}$$

where δF_+ (δB_+) and δF_- (δB_-) represent the forward- (backward-) going perturbation fields that are $\hat{\sigma}_+$ and $\hat{\sigma}_-$ polarized, respectively.

The details of the temporal stability analysis of the steady-state solution (13) are given in part 3 of the Appendix. The results for the amplitude stability are shown in Fig. 3 for the case of equal input intensities $I_f=I_b=I$. In order to make a direct comparison with the results of

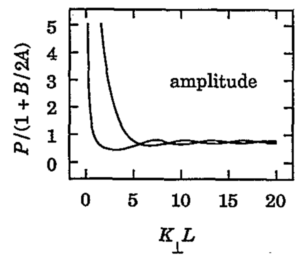

FIG. 3. Threshold intensity P rescaled by the factor $(1+B/2A)$ for the circular and corotating eigenpolarization configuration plotted as a function of the transverse wave-vector parameter $K_\perp L$ for the amplitude instability. The polarization for this configuration is predicted to be always temporally stable. Equal input intensities for the forward- and backward-traveling waves are assumed.

the linearly polarized eigenpolarization configuration, the normalized intensity P is defined in the same manner [i.e., $P=k(A'+B'/2)IL$] as the linear case. The result for the threshold intensity as a function of $K_\perp L$ is identical to the result from the amplitude stability analysis for the linear and parallel eigenpolarization configuration except that the threshold intensity depends on the ratio of B/A through the normalization factor $(1+B/2A)$. This factor occurs because the couplings between all the amplitude perturbations depend only on the coefficient A rather than $(A+B/2)$. The threshold value for phase-conjugate oscillation is also renormalized in the same manner and is given by $P_\infty=(1+B/2A)\pi/2$. The results of the polarization instability analysis reveal that the steady-state solutions (13) are always temporally stable to polarization perturbations. Thus the circular and corotating eigenpolarization configuration offers the best possibility of studying the scalar wave instabilities without any of the complications introduced by polarization effects. However, if the medium is allowed to have a noninstantaneous response (i.e., $\partial\chi_{ij}/\partial t\neq 0$), then polarization instabilities may also occur [27].

We finally consider the temporal stability of the circular and counterrotating eigenpolarization configuration. The steady-state solutions for the four field components for the case in which the incident forward and backward waves are $\hat{\sigma}_+$ and $\hat{\sigma}_-$ polarized, respectively, are given by

$$F_+^{\rm SS}(z)=\sqrt{I_f}\exp\{ik[A'I_f+(A'+B')I_b]z\}\ , \qquad (15a)$$

$$B_-^{\rm SS}(z)=\sqrt{I_b}\exp\{-ik[(A'+B')I_f+A'I_b]z\}\ , \qquad (15b)$$

$$F_-^{\rm SS}(z)=0\ , \qquad (15c)$$

$$B_+^{\rm SS}(z)=0\ , \qquad (15d)$$

where $I_f=(nc/2\pi)|F_+^{\rm SS}(0)|^2$ and $I_b=(nc/2\pi)|B_-^{\rm SS}(L)|^2$ are the input intensities of the forward and backward waves, respectively. We perturb the steady-state solution (15) by assuming that the total field inside the medium is given by

$$\begin{aligned}\mathbf{E}(\mathbf{r},t)=&\{[F_+^{\rm SS}(z)+\delta F_+(\mathbf{r}_\perp,z,t)]\hat{\sigma}_+\\ &+\delta F_-(\mathbf{r}_\perp,z,t)\hat{\sigma}_-\}e^{i(kz-\omega t)}\\ &+\{\delta B_+(\mathbf{r}_\perp,z,t)\hat{\sigma}_+\\ &+[B_-^{\rm SS}(z)+\delta B_-(\mathbf{r}_\perp,z,t)]\hat{\sigma}_-\}e^{i(-kz-\omega t)}\ .\end{aligned} \qquad (16)$$

The details of the stability analysis are given in part 4 of the Appendix and the results are shown for the case of equal input intensities in Fig. 4 for $B/A=6$ [Figs. 4(a) and 4(d)], 1 [Figs. 4(b) and 4(e)], and 0 [Figs. 4(c) and 4(f)]. Similar to the results for the amplitude-stability analysis of the other eigenpolarizations, we find that the threshold for the amplitude instability is infinite on axis in all three cases [Figs. 4(a)–4(c)]. The minimum value of P is found to decrease slightly for increasing values of B/A, and for the three values of B/A shown it occurs at $K_\perp L\approx 3$. The minimum threshold values are given by $P\approx 0.8$, 0.7, and 0.6 for $r=0$, 1, and 6, respectively. In all cases the values are below the threshold $P_\infty=(1+B/2A)\pi/2(1+B/A)$ for phase-conjugate oscillation. The threshold intensity for the polarization instability [Figs. 4(d)–4(f)] is found to be independent of $K_\perp L$ for all values of r and is simply equal to the corresponding threshold intensity P_∞ for phase-conjugate oscillation, which for all cases is given by the respective value of P_∞ for the amplitude perturbations. In all cases shown the threshold intensity for the amplitude instability is lower than the value for the polarization instability.

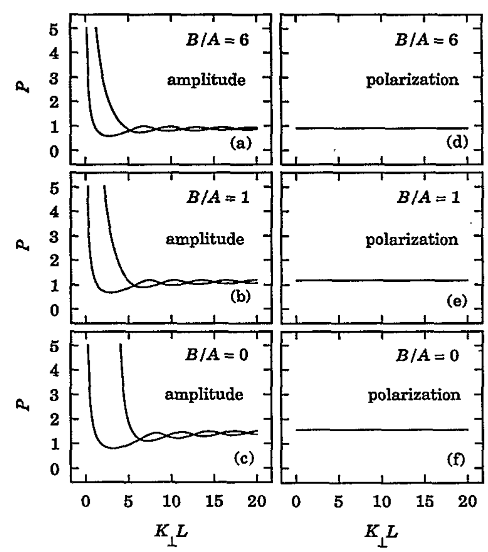

FIG. 4. Normalized threshold intensity P for the circular and counterrotating eigenpolarization configuration plotted as a function of the transverse wave-vector parameter $K_\perp L$ for (a)–(c) the amplitude instability and (d)–(f) the polarization instability for (a) and (d) $B/A=6$, (b) and (e) $B/A=1$, and (c) and (f) $B/A=0$. Equal input intensities for the forward- and backward-traveling waves are assumed.

NUMERICAL INTEGRATION OF COUPLED NONLINEAR EQUATIONS

For most of the results of the stability analysis shown here, the threshold for the amplitude instability is somewhat lower than the threshold for the polarization instability for a particular value of the ratio of B/A. This result could lead one to believe that polarization effects are not important in the instability regime. Nevertheless, we believe that the inclusion of polarization effects is critical to the determination of the full dynamics of the system in the instability regime. In Fig. 5 we give an example of a numerical integration of the full coupled nonlinear equations for the case of the linear and parallel eigenpolarization configuration with $B/A=6$ in the regime in which the input intensity $P^{\text{in}}=0.7$ of the two input waves is above the threshold for the amplitude instability [$P=0.45$; see Fig. 1(a)] but below the threshold for the corresponding polarization instability [$P=0.8$; see Fig. 1(c)]. As a result of the computing-insensitive nature of the integration, we have considered only a single transverse dimension (i.e., x direction). The split-step fast-Fourier-transform method [29] of integration along the characteristics is used to perform the integration. The transverse profile of the input files is assumed to be Gaussian such that

$$F_x(x,0,t)=B_x(x,L,t)=\left[\frac{2\pi P^{\text{in}}}{nck(A+B/2)L}\right]^{1/2} e^{-x^2/w_0^2} \tag{17}$$

with a beam radius corresponding to a confocal parameter that is given by $kw_0^2/L=400$. We also assume that in the input field of the forward-traveling wave that there is a small constant field polarized along the y direction with a magnitude equal to $10^{-5}P^{\text{in}}$. In Figs. 5(a) and 5(b), we plot the normalized output intensity $P_{i=x,y}^{\text{out}}(x=0)=(nc/2\pi)k(A'+B'/2)|F_i(0,L,t)|^2L$ of the forward-going wave as a function of time at the center (i.e., $x=0$) of the transverse profile for the field polarized along the x and y directions, respectively. The fields are ramped on smoothly to the corresponding steady-state input value within five transit times. The amplitude of the field initially becomes unstable after approximately 25 transit times. After approximately 55 transit times the polarization also becomes unstable. For the time duration shown here, the system does not settle to a stable steady state. Figures 6(a) and 6(b) show the transverse intensity profiles of the x- and y-polarized components of the output of the forward-traveling wave at 150 transit times. The transverse profiles of each component show deep modulation with the width of the y-polarization component being nominally half the width w_0 of the input field. Since the system does not settle to a steady state, the transverse profiles continue to change as is evidenced by the transverse profiles of the transmitted wave at 300 transit times [Figs. 6(c) and 6(d) for the x- and y-polarized components, respectively].

Further numerical studies for very long times would be necessary to determine if the system ever reaches a stable steady-state value. Also, an integration that includes both transverse dimensions would be needed to determine the true dynamical behavior of counterpropagating laser beams such as pattern formation [26]. However, we believe that the numerical results shown here present strong evidence that the inclusion of the tensor properties of this interaction is important in determining the full dynamical behavior of the system. We expect that the cases in which the scalar treatment of counterpropagating waves is fully valid are for the circular and corotating configuration and for the linear and parallel configuration with $B/A=0$, since in these cases the threshold for polarization instability is infinite.

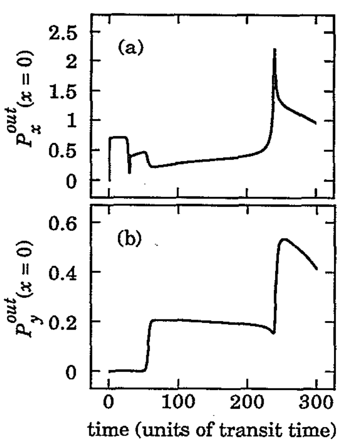

FIG. 5. Temporal evolution of the intensity at the center [i.e., $x=0$] of the transverse profile of the (a) x and (b) y components of the transmitted forward-going wave. The ratio of $B/A=6$ and the normalized input intensities are equal and given by the value of $P^{\text{in}}=0.7$, which is above the threshold for the amplitude instability, but below the threshold for the corresponding polarization instability. Both the amplitude and the polarization of the output field exhibit temporal fluctuations.

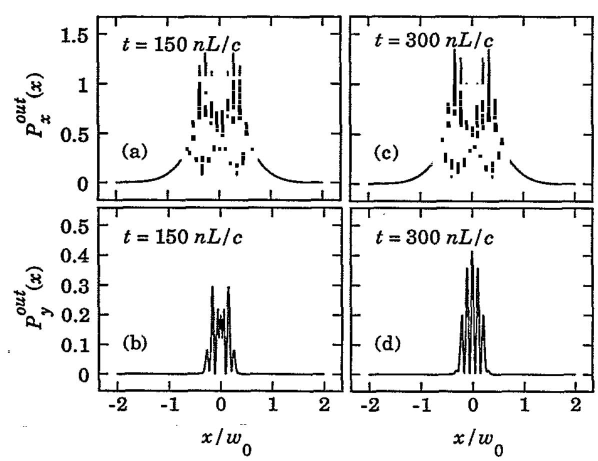

FIG. 6. Transverse intensity profile of the (a) and (c) x and (b) and (d) y components of the transmitted forward-going wave after (a) and (b) 150 transit times and (c) and (d) 300 transit times for the conditions described in Fig. 5. The transverse profiles of both the amplitude and the polarization of the field exhibit deep modulation.

TABLE I. Summary of the result of the linear stability analyses for $I_f = I_b$.

Eigenpolarization	Temporal stability
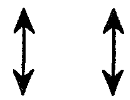	Lowest instability threshold is for amplitude instability and occurs off axis at $K_\perp L \approx 3$.
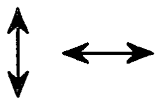	For $B/A = 0$, lowest instability threshold is for amplitude instability and occurs off axis at $K_\perp L \approx 3$. For $B/A = 1$, lowest instability threshold is for amplitude instability and occurs off axis at $K_\perp L \approx 3$. For $B/A = 6$, lowest instability threshold is for polarization instability and occurs on axis.
	Polarization is always stable. Amplitude can become unstable, and the lowest instability threshold occurs off axis at $K_\perp L \approx 3$
	Lowest instability threshold is for amplitude instability and occurs off axis at $K_\perp L \approx 3$ for $B/A = 0$, 1, or 6.

CONCLUSIONS

We have investigated the transverse stability of the amplitudes and the polarizations of the four eigenpolarization configurations of counterpropagating waves in an isotropic medium. The results of the stability analysis are summarized by Table I. We find that in most cases the amplitudes of the fields become unstable at lower threshold intensities than do the polarizations, and that except for the case of linear and parallel configuration, the tensor properties of the medium (i.e., the ratio B/A) determine the threshold for instability for the amplitudes of the waves. We also find through numerical integration of the full nonlinear equations with one transverse dimension that the polarizations of the fields can become unstable for input intensities that are below the threshold for the polarization instability but above the threshold for the amplitude instability as calculated from linear stability analysis. We thus conclude that, in general, consideration of the tensor properties of the nonlinear interaction is important in describing the dynamical behavior of counterpropagating waves.

ACKNOWLEDGMENTS

The work was supported by the U.S. Army Research Office through the University Research Initiative and by the New York State Center for Advanced Optical Technology.

APPENDIX

In order to determine the amplitude and polarization stability of the four mutual eigenpolarizations, we perform a stability analysis on the respective steady-state solutions.

1. Linear and parallel

We perturb the amplitude and the polarization of the steady-state fields by assuming that the total field is given by

$$\mathbf{E}(\mathbf{r},t) = \{[F_x^{SS}(z) + \delta F_x(\mathbf{r}_\perp,z,t)]\hat{\mathbf{x}} + \delta F_y(\mathbf{r}_\perp,z,t)\hat{\mathbf{y}}\}e^{i(kz-\omega t)} + \{[B_x^{SS}(z) + \delta B_x(\mathbf{r}_\perp,z,t)]\hat{\mathbf{x}} + \delta B_y(\mathbf{r}_\perp,z,t)\hat{\mathbf{y}}\}e^{i(-kz-\omega t)} \quad \text{(A1)}$$

where δF_x (δB_x) and δF_y (δB_y) represent forward- (backward-) going perturbation field polarized along the x and y directions, respectively. We assume that these perturbations have the following form:

$$\delta F_x(z,t) = [f_x^S(z)e^{\lambda t} + f_x^a e^{\lambda^* t}]e^{i\mathbf{k}_\perp \cdot \mathbf{r}_\perp}, \quad \text{(A2a)}$$

$$\delta B_x(\mathbf{r}_\perp,z,t) = [b_x^S(z)e^{\lambda t} + b_x^a e^{\lambda^* t}]e^{i\mathbf{k}_\perp \cdot \mathbf{r}_\perp}, \quad \text{(A2b)}$$

$$\delta F_y(\mathbf{r}_\perp,z,t) = [f_y^S(z)e^{\lambda t} + f_y^a e^{\lambda^* t}]e^{i\mathbf{k}_\perp \cdot \mathbf{r}_\perp}, \quad \text{(A2c)}$$

$$\delta B_y(\mathbf{r}_\perp,z,t) = [b_y^S(z)e^{\lambda t} + b_y^a e^{\lambda^* t}]e^{i\mathbf{k}_\perp \cdot \mathbf{r}_\perp}. \quad \text{(A2d)}$$

By assuming this form, one can interpret for the case $\text{Im}(\lambda) > 0$ the amplitudes f_i^S and b_i^S ($i = x,y$) as being the forward- and backward-traveling Stokes components, respectively, and f_i^a and b_i^a ($i = x,y$) as being the forward- and backward-traveling anti-Stokes components, respectively. As a result of the four-wave interaction, the Stokes and anti-Stokes components are coupled, and thus both these components must be present in the assumed form for the perturbation. We substitute the electric field into Eqs. (4) and (5) and linearize the resulting equations for the perturbation amplitudes. We find that the perturbation amplitudes polarized along the x direction decouple from the amplitudes polarized along the y direction, which yields the following equations for the perturbation polarized along the x direction:

$$\frac{df_x^S}{dz}=\left[-\frac{\lambda}{c}-iK_\perp+i(2A'+B')(I_f+I_b)\right]f_x^S+i(2A'+B')\left[\frac{nc}{2\pi}F_x^S B_x^{SS*}\right]b_x^S+i\left[A'+\frac{B'}{2}\right]\left[\frac{nc}{2\pi}F_x^{SS2}\right]f_x^{a*}+i(2A'+B')\left[\frac{nc}{2\pi}F_x^{SS}B_x^{SS}\right]b_x^{a*}\,, \tag{A3a}$$

$$\frac{db_x^S}{dz}=\left[\frac{\lambda}{c}+iK_\perp-i(2A'+B')(I_f+I_b)\right]b_x^S-i(2A'+B')\left[\frac{nc}{2\pi}F_x^{SS*}B_x^{SS}\right]f_x^S-i(2A'+B')\left[\frac{nc}{2\pi}F_x^{SS}B_x^{SS}\right]f_x^{a*}-i\left[A'+\frac{B'}{2}\right]\left[\frac{nc}{2\pi}B_x^{SS2}\right]b_x^{a*}\,, \tag{A3b}$$

$$\frac{df_x^{a*}}{dz}=-\left[\frac{\lambda}{c}-iK_\perp+i(2A'+B')(I_f+I_b)\right]f_x^{a*}-i(2A'+B')\left[\frac{nc}{2\pi}F_x^{SS*}B_x^{SS}\right]b_x^{a*}-i\left[A'+\frac{B'}{2}\right]\left[\frac{nc}{2\pi}F_x^{SS*2}\right]f_x^S-i(2A'+B')\left[\frac{nc}{2\pi}F_x^{SS*}B_x^{SS*}\right]b_x^S\,, \tag{A3c}$$

$$\frac{db_x^{a*}}{dz}=\left[\frac{\lambda}{c}-iK_\perp+i(2A'+B')(I_fI_b)\right]b_x^{a*}+i(2A'+B')\left[\frac{nc}{2\pi}F_x^{SS}B_x^{SS*}\right]f_x^{a*}+i(2A'+B')\left[\frac{nc}{2\pi}F_x^{SS*}B_x^{SS*}\right]f_x^S+i\left[A'+\frac{B'}{2}\right]\left[\frac{nc}{2\pi}B_x^{SS*2}\right]b_x^S \tag{A3d}$$

and for the perturbations polarized along the y direction

$$\frac{df_y^S}{dz}=\left[-\frac{\lambda}{c}-iK_\perp+iA'(I_f+I_b)\right]f_y^S+iA'\left[\frac{nc}{2\pi}F_x^{SS}B_x^{SS*}\right]b_y^S+\frac{i}{2}B'\left[\frac{nc}{2\pi}F_x^{SS2}\right]f_y^{a*}+iB'\left[\frac{nc}{2\pi}F_x^{SS}B_x^{SS}\right]b_y^{a*}\,, \tag{A4a}$$

$$\frac{db_y^S}{dz}=\left[\frac{\lambda}{c}+iK_\perp-iA'(I_f+I_b)\right]b_y^S-iA'\left[\frac{nc}{2\pi}F_x^{SS*}B_x^{SS}\right]f_y^S-iB'\left[\frac{nc}{2\pi}F_x^{SS}B_x^{SS}\right]f_y^{a*}-\frac{i}{2}B'\left[\frac{nc}{2\pi}B_x^{SS2}\right]b_y^{a*}\,, \tag{A4b}$$

$$\frac{df_y^{a*}}{dz}=\left[-\frac{\lambda}{c}+iK_\perp-iA'(I_f+I_b)\right]f_y^{a*}-iA'\left[\frac{nc}{2\pi}F_x^{SS*}B_x^{SS}\right]b_y^{a*}-\frac{i}{2}B'\left[\frac{nc}{2\pi}F_x^{SS*2}\right]f_y^S-iB'\left[\frac{nc}{2\pi}F_x^{SS*}B_x^{SS*}\right]b_y^S\,, \tag{A4c}$$

$$\frac{db^{a*}}{dz}=\left[\frac{\lambda}{c}-iK_\perp+iA'(I_f+I_b)\right]b_y^{a*}+iA'\left[\frac{nc}{2\pi}F_x^S B_x^{SS*}\right]f_y^{a*}+iB'\left[\frac{nc}{2\pi}F_x^{SS*}B_x^{SS*}\right]f_y^S+\frac{i}{2}B'\left[\frac{nc}{2\pi}B_x^{SS*2}\right]b_y^S \tag{A4d}$$

where $I_f=(nc/2\pi)|F_x^{SS}(0)|^2$ and $I_b=(nc/2\pi)|B_x^{SS}(L)|^2$ are the input intensities, $A'=4\pi^2\omega A/(nc)^2$ and $B'=4\pi^2\omega B/(nc)^2$ are the rescaled nonlinear coefficients, and $K_\perp=(k_x^2+k_y^2)/2k$ is the transverse wave-vector parameter.

We solve each set of equations for the perturbation amplitudes by first substituting the steady-state solutions for F_x^{SS} and B_x^{SS} and by making the following transformation of the amplitudes:

$$f_j^i(z)=\tilde{f}_j^i(z)\exp\left[i\left[A'+\frac{B'}{2}\right](I_f+2I_b)z\right]\,, \tag{A5a}$$

$$b_j^i(z)=\tilde{b}_j^i(z)\exp\left[-i\left[A'+\frac{B'}{2}\right](2I_f+I_b)z\right] \tag{A5b}$$

where $i=S,a$ and $j=x,y$. We express the resulting equation for the $\tilde{f}_j^i$ and $\tilde{b}_j^i$ in matrix form

$$\frac{d}{dz/L}\begin{bmatrix}\tilde{f}_x^S\\ \tilde{b}_x^S\\ \tilde{f}_x^{a*}\\ \tilde{b}_x^{a*}\end{bmatrix}=\begin{bmatrix}-\lambda T_t-iK_\perp L+i2P_f & i2\sqrt{P_fP_b} & iP_f & i2\sqrt{P_fP_b}\\ -i2\sqrt{P_fP_b} & \lambda T_t+iK_\perp L-i2P_b & -i2\sqrt{P_fP_b} & -iP_b\\ -iP_f & -i2\sqrt{P_fP_b} & -\lambda T_t+iK_\perp L-i2P_f & -i2\sqrt{P_fP_b}\\ i2\sqrt{P_fP_b} & iP_b & i2\sqrt{P_fP_b} & \lambda T_t-iK_\perp L+i2P_b\end{bmatrix}\begin{bmatrix}\tilde{f}_x^S\\ \tilde{b}_x^S\\ \tilde{f}_x^{a*}\\ \tilde{b}_x^{a*}\end{bmatrix}, \tag{A6}$$

$$\frac{d}{dz/L}\begin{bmatrix}\tilde{f}_y^S\\ \tilde{b}_y^S\\ \tilde{f}_y^{a\,*}\\ \tilde{b}_y^{a\,*}\end{bmatrix}=\begin{bmatrix}-\lambda T_t-i[K_\perp L+\frac{r}{2}P'_f+(1+r)P'_b] & i\sqrt{P'_fP'_b} & \frac{i}{2}rP'_f & ir\sqrt{P'_fP'_b}\\ -i\sqrt{P'_fP'_b} & \lambda T_t+i[K_\perp L+(1+r)P'_f+\frac{r}{2}P'_b] & -ir\sqrt{P'_fP'_b} & -\frac{i}{2}rP'_b\\ -\frac{i}{2}rP'_f & -ir\sqrt{P'_fP'_b} & -\lambda T_t+i[K_\perp L+\frac{r}{2}P'_f+(1+r)P'_b] & -i\sqrt{P'_fP'_b}\\ ir\sqrt{P'_fP'_b} & \frac{i}{2}rP'_b & i\sqrt{P'_fP'_b} & \lambda T_t-i[K_\perp L+(1+kr)P'_f+\frac{r}{2}P'_b]\end{bmatrix}\begin{bmatrix}\tilde{f}_y^S\\ \tilde{b}_y^S\\ \tilde{f}_y^{a\,*}\\ \tilde{b}_y^{a\,*}\end{bmatrix} \quad \text{(A7)}$$

where $P_{f,b}=(A'+B'/2)I_{f,b}L$ are the normalized input intensities of the forward and backward waves, $r=B/A$ is the ratio of the nonlinear coefficients, $T_t=L/c$ is the transit time through the medium, and $P'_{f,b}=P_{f,b}/(1+r/2)$. Since the elements of the 4×4 matrices above are all constants, solving for the perturbation amplitudes becomes an eigenvalue problem. We thus proceed with the stability analysis as follows by considering the perturbation amplitudes polarized along the x direction. The analysis for the perturbation amplitudes polarized along the y direction are treated analogously. The solution to the set of equations can be expressed as

$$\begin{bmatrix}\tilde{f}_x^S(z)\\ \tilde{b}_x^S(z)\\ \tilde{f}_x^a(z)\\ \tilde{b}_x^a(z)\end{bmatrix}=\begin{bmatrix}\zeta_1^{Sf} & \zeta_2^{Sf} & \zeta_3^{Sf} & \zeta_4^{Sf}\\ \zeta_1^{Sb} & \zeta_2^{Sb} & \zeta_3^{Sb} & \zeta_4^{Sb}\\ \zeta_1^{af} & \zeta_2^{af} & \zeta_3^{af} & \zeta_4^{af}\\ \zeta_1^{ab} & \zeta_2^{ab} & \zeta_3^{ab} & \zeta_4^{ab}\end{bmatrix}\begin{bmatrix}C_1e^{\gamma_1 z}\\ C_2e^{\gamma_2 z}\\ C_3e^{\gamma_3 z}\\ C_4e^{\gamma_4 z}\end{bmatrix} \quad \text{(A8)}$$

where the γ_i's are the eigenvalues of matrix (A6), the ζ_i^{jk}'s ($j=S,a$; $k=f,b$) are the associated eigenvectors, and the C_i's are the constants which are determined by the boundary conditions. For the stability analysis, we apply the boundary conditions $\tilde{f}_x^S(0)=\tilde{b}_x^S(L)=\tilde{f}_x^{a\,*}(0)=\tilde{b}_x^{a\,*}(L)=0$, which leads to the following condition:

$$\begin{bmatrix}\zeta_1^{Sf} & \zeta_2^{Sf} & \zeta_3^{Sf} & \zeta_4^{Sf}\\ \zeta_1^{Sb}e^{\gamma_1 L} & \zeta_2^{Sb}e^{\gamma_2 L} & \zeta_3^{Sb}e^{\gamma_3 L} & \zeta_4^{Sb}e^{\gamma_4 L}\\ \zeta_1^{af} & \zeta_2^{af} & \zeta_3^{af} & \zeta_4^{af}\\ \zeta_1^{ab}e^{\gamma_1 L} & \zeta_2^{ab}e^{\gamma_2 L} & \zeta_3^{ab}e^{\gamma_3 L} & \zeta_4^{ab}e^{\gamma_4 L}\end{bmatrix}\begin{bmatrix}C_1\\ C_2\\ C_3\\ C_4\end{bmatrix}=0\,, \quad \text{(A9a)}$$

$$\underline{M}_3\begin{bmatrix}C_1\\ C_2\\ C_3\\ C_4\end{bmatrix}=0\,. \quad \text{(A9b)}$$

In order to reach a nontrivial solution (i.e., $\{C\}\neq 0$), the determinant of $\underline{M}_3$ must vanish,

$$\det(\underline{M}_3)=0\,. \quad \text{(A10)}$$

For a fixed ratio of I_b/I_f and of B/A, the condition above (A10) results in a complex transcendental equation involving both λ and the total normalized intensity $P_T=P_f+P_b$. By setting $\mathrm{Re}(\lambda)=0$, we solve the real and imaginary parts of the resulting transcendental equation for the oscillation frequency $\Delta=\mathrm{Im}(\lambda)T_t$ and the intensity P_T at the threshold for instability.

2. Linear and perpendicular

We perturb the amplitudes and the polarizations of the steady-state fields by assuming that the total field is given by

$$\mathbf{E}(\mathbf{r},t)=\{[F_x^{\rm SS}(z)+\delta F_x(\mathbf{r}_\perp,z,t)]\hat{\mathbf{x}}+\delta F_y(\mathbf{r}_\perp,z,t)\hat{\mathbf{y}}\}e^{i(kz-wt)}+\{\delta B_x(\mathbf{r}_\perp,z,t)\hat{\mathbf{x}}+[B_y^{\rm SS}(z)+\delta B_y(\mathbf{r}_\perp,z,t)]\hat{\mathbf{y}}\}e^{i(-kz-wt)}\ . \tag{A11}$$

We assume that the perturbations have the form given by Eqs. (A2), and we find that the perturbation amplitudes also decouple into two sets of four equations. As in the case of linear and parallel input fields, the amplitude perturbations of the forward and backward fields couple with one another, and the polarization perturbations couple with one another. The resulting linearized equations for the amplitude-perturbation fields are given by

$$\frac{df_x^S}{dz}=\left[-\frac{\lambda}{c}-iK_\perp+i(2A'+B')I_f+iA'I_b\right]f_x^S+iA'\left[\frac{nc}{2\pi}F_x^{\rm SS}B_y^{\rm SS*}\right]b_y^S+i\left[A'+\frac{B'}{2}\right]\left[\frac{nc}{2\pi}F_x^{\rm SS2}\right]f_x^{a*}+iA\left[\frac{nc}{2\pi}F_x^{\rm SS}B_y^{\rm SS}\right]b_y^{a*}\ , \tag{A12a}$$

$$\frac{db_y^S}{dz}=\left[\frac{\lambda}{c}+iK_\perp-iA'I_f-i(2A'+B')I_b\right]b_y^S+iA'\left[\frac{nc}{2\pi}F_x^{\rm SS}B_y^{\rm SS}\right]f_x^S-iA'\left[\frac{nc}{2\pi}F_x^{\rm SS}B_y^{\rm SS}\right]f_x^{a*}-i\left[A'+\frac{B'}{2}\right]\left[\frac{nc}{2\pi}B_y^{\rm SS2}\right]b_y^{a*}\ , \tag{A12b}$$

$$\frac{df_x^{a*}}{dz}=-\left[\frac{\lambda}{c}-iK_\perp+i(2A'+B')I_f+iA'I_b\right]f_x^{a*}-iA\left[\frac{nc}{2\pi}F_x^{S*}B_y^{\rm SS}\right]b_y^{a*}-i\left[A'+\frac{B'}{2}\right]\left[\frac{nc}{2\pi}F_x^{\rm SS*2}\right]f_x^S-iA'\left[\frac{nc}{2\pi}F_x^{\rm SS*}B_y^{\rm SS*}\right]b_y^S\ , \tag{A12c}$$

$$\frac{db_y^{a*}}{dz}=\left[\frac{\lambda}{c}-iK_\perp+iA'I_f+i(2A'+B')I_b\right]b_y^{a*}+iA'\left[\frac{nc}{2\pi}F_x^{\rm SS}B_y^{\rm SS*}\right]f_x^{a*}+iA'\left[\frac{nc}{2\pi}F_x^{\rm SS*}B_y^{\rm SS*}\right]f_x^S+i\left[A'+\frac{B'}{2}\right]\left[\frac{nc}{2\pi}B_y^{\rm SS*2}\right]b_y^S \tag{A12d}$$

and for the polarization-perturbation fields

$$\frac{df_y^S}{dz}=\left[-\frac{\lambda}{c}-iK_\perp+iA'I_f+i(2A'+B')I_b\right]f_y^S+i\frac{B'}{2}\left[\frac{nc}{2\pi}F_x^{\rm SS}B_y^{\rm SS*}\right]b_x^S+i\frac{B'}{2}\left[\frac{nc}{2\pi}F_x^{\rm SS*2}\right]f_y^{a*}+i\left[A'-\frac{B'}{2}\right]\left[\frac{nc}{2\pi}F_x^{\rm SS}B_y^{\rm SS}\right]b_x^{a*}\ , \tag{A13a}$$

$$\frac{db_x^S}{dz}=\left[\frac{\lambda}{c}+iK_\perp-i(2A'+B')I_f-iA'I_b\right]b_x^S-i\frac{B'}{2}\left[\frac{nc}{2\pi}F_x^{\rm SS*}B_y^{\rm SS}\right]f_y^S-i\left[A'-\frac{B'}{2}\right]\left[\frac{nc}{2\pi}F_x^{\rm SS}B_y^{\rm SS}\right]f_y^{a*}-i\frac{B}{2}\left[\frac{nc}{2\pi}B_y^{\rm SS2}\right]b_x^{a*}\ , \tag{A13b}$$

$$\frac{df_y^{a*}}{dz}=-\left[\frac{\lambda}{c}-iK_\perp+iA'I_f+i(2A'+B')I_b\right]f_y^{a*}-i\frac{B'}{2}\left[\frac{nc}{2\pi}F_x^{\rm SS*}B_y^{\rm SS}\right]b_x^{a*}-i\frac{B}{2}\left[\frac{nc}{2\pi}F_x^{\rm SS*2}\right]f_y^S-i\left[A'-\frac{B'}{2}\right]\left[\frac{nc}{2\pi}F_x^{\rm SS*}B_x^{\rm SS*}\right]b_x^S\ , \tag{A13c}$$

$$\frac{db_x^{a*}}{dz}=\left[\frac{\lambda}{c}-iK_\perp+i(2A'+B')I_f+iAI_b\right]b_x^{a*}+i\frac{B'}{2}\left[\frac{nc}{2\pi}F_x^{\rm SS*}B_y^{\rm SS*}\right]f_y^{a*}+i\left[A'-\frac{B'}{2}\right]\left[\frac{nc}{2\pi}F_x^{\rm SS*}B_y^{\rm SS*}\right]f_y^S+i\frac{B'}{2}\left[\frac{nc}{2\pi}B_x^{\rm SS*2}\right]b_x^S\ . \tag{A13d}$$

As we did previously for the case of linear and parallel inputs, we make a transformation of the amplitudes so that we can put the equations in matrix form which can be easily solved,

$$f_j^i(z)=\tilde{f}_j^i(z)\exp\left\{i\left[\left[A'+\frac{B'}{2}\right]I_f+A'I_b\right]z\right\}\ , \tag{A14a}$$

$$b_j^i(z)=\tilde{b}_j^i(z)\exp\left\{-i\left[A'I_f+\left[A'+\frac{B'}{2}\right]I_f\right]z\right\} \tag{A14b}$$

where $i=S,a$ and $j=x,y$. Thus the equations for the $\tilde{f}_j^i$'s and the $\tilde{b}_j^i$'s become

$$\frac{d}{dz/L}\begin{bmatrix}\tilde{f}_x^S\\ \tilde{b}_y^S\\ \tilde{f}_x^{a*}\\ \tilde{b}_y^{a*}\end{bmatrix}=\begin{bmatrix}-\lambda T_t-iK_\perp L+iP_f & i\sqrt{P_f'P_b'} & iP_f & i\sqrt{P_f'P_b'}\\ -i\sqrt{P_f'P_b'} & \lambda T_t+iK_\perp L-iP_b & -i\sqrt{P_f'P_b'} & -iP_b\\ -iP_f & -i\sqrt{P_f'P_b'} & -\lambda T_t+iK_\perp L-iP_f & -i\sqrt{P_f'P_b'}\\ i\sqrt{P_f'P_b'} & iP_b & i\sqrt{P_f'P_b'} & \lambda T_t-iK_\perp L+iP_b\end{bmatrix}\begin{bmatrix}\tilde{f}_x^S\\ \tilde{b}_y^S\\ \tilde{f}_x^{a*}\\ \tilde{b}_y^{a*}\end{bmatrix}, \quad \text{(A15)}$$

and see Eq. (A16) on the following page.

The procedure for the stability analysis is analogous to that for the amplitude perturbation with linear and parallel inputs.

3. Circular and corotating

In the circularly polarized basis, we perturb the amplitude and polarization of the steady-state fields by assuming that the total field is given by

$$\mathbf{E}(\mathbf{r},t)=\{[F_+^{\rm SS}(z)+\delta F_+(\mathbf{r}_\perp,z,t)]\hat{\sigma}_+ +\delta F_-(\mathbf{r}_\perp,z,t)\hat{\sigma}_-\}e^{i(kz-\omega t)} +\{[B_+^{\rm SS}(z)+\delta B_+(\mathbf{r}_\perp,z,t)]\hat{\sigma}_+ +\delta B_-(\mathbf{r}_\perp,z,t)\hat{\sigma}_-\}e^{i(-kz-\omega t)} \quad \text{(A17)}$$

where δF_+ (δB_+) and δF_- (δB_-) represent the forward- (backward-) going perturbation fields that are $\hat{\sigma}_+$ and $\hat{\sigma}_-$ polarized, respectively. As with the linearly polarized input polarizations, we assume that the perturbation fields have the form

$$\delta F_+(\mathbf{r}_\perp,z,t)=[f_+^S(z)e^{\lambda t}+f_+^a e^{\lambda^* t}]e^{i\mathbf{k}_\perp\cdot\mathbf{r}_\perp}, \quad \text{(A18a)}$$

$$\delta B_+(\mathbf{r}_\perp,z,t)=[b_+^S(z)e^{\lambda t}+b_+^a e^{\lambda^* t}]e^{i\mathbf{k}_\perp\cdot\mathbf{r}_\perp}, \quad \text{(A18b)}$$

$$\delta F_-(\mathbf{r}_\perp,z,t)=[f_-^S(z)e^{\lambda t}+f_-^a(z) e^{\lambda^* t}]e^{i\mathbf{k}_\perp\cdot\mathbf{r}_\perp}, \quad \text{(A18c)}$$

$$\delta B_-(\mathbf{r}_\perp,z,t)=[b_-^S(z)e^{\lambda t}+b_-^a(z) e^{\lambda^* t}]e^{i\mathbf{k}_\perp\cdot\mathbf{r}_\perp}. \quad \text{(A18d)}$$

By substituting the field $\mathbf{E}$ into Eqs. (4) and (12) and linearizing the resulting equations for the perturbation amplitudes f_j^i's and b_j^i's, we find that the amplitude and polarization perturbations decouple into two sets of differential equations. The set of equations for the amplitude-perturbation fields is identical to those [Eqs. (A3)] for the amplitude-perturbation fields for the linear and parallel eigenpolarization with the substitution of A' for $A'+B'/2$, + for x, and − for y.

The set of equations for the polarization-perturbation fields further decouples into two sets of two equations in which only the Stokes (anti-Stokes) components are coupled. The resulting equations for the Stokes components are given by

$$\frac{df_-^S}{dz}=\left[-\frac{\lambda}{c}-iK_\perp+i(A'+B')(I_f+I_b)\right]f_-^S +i(A'+B')\left[\frac{nc}{2\pi}F_+^{\rm SS}B_+^{\rm SS*}\right]b_-^S, \quad \text{(A19a)}$$

$$\frac{db_-^S}{dz}=\left[\frac{\lambda}{c}+iK_\perp-i(A'+B')(I_f+I_b)\right]b_-^S -i(A'+B')\left[\frac{nc}{2\pi}F_+^{\rm SS}B_+^{\rm SS*}\right]f_-^S \quad \text{(A19b)}$$

where $I_f=(nc/2\pi)|F_+^{\rm SS}(0)|^2$ and $I_b=(nc/2\pi)|B_+^{\rm SS}(L)|^2$ are the input intensities. The equations for f_-^a and b_-^a are entirely equivalent to those above with the replacement of f_-^a for f_-^S, b_-^a for b_-^S, and λ^* for λ.

We transform the amplitudes through the relations

$$f_j^i(z)=\tilde{f}_j^i(z)\exp[iA'(I_f+2I_b)z], \quad \text{(A20a)}$$

$$b_j^i(z)=\tilde{b}_j^i(z)\exp[-iA'(2I_f+I_b)z] \quad \text{(A20b)}$$

where $i=S,a$ and $j=+,-$. The resulting equations in matrix form are given by

$$\frac{d}{dz/L}\begin{bmatrix}\tilde{f}_-^S\\ \tilde{b}_-^S\end{bmatrix}=\begin{bmatrix}-\lambda T_t-iK_\perp L+irP_f'-i(1-r)P_b' & i(1+r)\sqrt{P_f'P_b'}\\ -i(1+r)\sqrt{P_f'P_b'} & \lambda T_t+iK_\perp L+i(1-r)P_f'-irP_b'\end{bmatrix}\begin{bmatrix}\tilde{f}_-^S\\ \tilde{b}_-^S\end{bmatrix}. \quad \text{(A21)}$$

The stability analysis is then completed in a manner analogous to that for the amplitude polarization field for the linear and parallel inputs.

4. Circular and counterrotating

We perturb the amplitudes and polarizations of the steady-state fields by assuming that the total field is given by

$$\mathbf{E}(\mathbf{r},t)=\{[F_+^{\rm SS}(z)+\delta F_+(\mathbf{r}_\perp,z,t)]\hat{\sigma}_+ +\delta F_-(\mathbf{r}_\perp,z,t)\hat{\sigma}_-\}e^{i(kz-\omega t)} +\{\delta B_+(\mathbf{r}_\perp,z,t)\hat{\sigma}_+ +[B_-^{\rm SS}(z)+\delta B_-(\mathbf{r}_\perp,z,t)]\hat{\sigma}_-\}e^{i(-kz-\omega t)}. \quad \text{(A22)}$$

$$\frac{d}{dz/L}\begin{bmatrix} \tilde{f}_y^S \\ \tilde{b}_x^S \\ \tilde{f}_y^{a*} \\ \tilde{b}_x^{a*} \end{bmatrix} = \begin{bmatrix} -\lambda T_t - i\left[K_\perp L+\frac{r}{2}P'_f-rP'_b\right] & i\frac{r}{2}\sqrt{P'_fP'_b} & i\frac{r}{2}P'_f & i\left[1-\frac{r}{2}\right]\sqrt{P'_fP'_b} \\ -i\frac{r}{2}\sqrt{P'_fP'_b} & \lambda T_t+i\left[K_\perp L-rP'_f+\frac{r}{2}P'_b\right] & -i\left[1-\frac{r}{2}\right]\sqrt{P'_fP'_b} & -i\frac{r}{2}P'_b \\ -i\frac{r}{2}P'_f & -i\left[1-\frac{r}{2}\right]\sqrt{P'_fP'_b} & -\lambda T_t+i\left[K_\perp L+\frac{r}{2}P'_f-rP'_b\right] & -i\frac{r}{2}\sqrt{P'_fP'_b} \\ i\left[1-\frac{r}{2}\right]\sqrt{P'_fP'_b} & i\frac{r}{2}P'_b & i\frac{r}{2}\sqrt{P'_fP'_b} & \lambda T_t-i\left[K_\perp L-rP'_f+\frac{r}{2}P'_b\right] \end{bmatrix} \begin{bmatrix} \tilde{f}_y^S \\ \tilde{b}_x^S \\ \tilde{f}_y^{a*} \\ \tilde{b}_x^{a*} \end{bmatrix} . \tag{A16}$$

As in all the previous cases, the linearized equations for the amplitude-perturbation fields decouple from those for the polarization-perturbation fields. The resulting equations for the amplitude perturbation fields are given by

$$\frac{df_+^S}{dz} = \left[-\frac{\lambda}{c} - iK_\perp + i2A'I_f + i(A'+B')I_b\right] f_+^S + i(A'+B')\left[\frac{nc}{2\pi}F_+^{\rm SS}B_-^{\rm SS*}\right] b_-^S + iA'\left[\frac{nc}{2\pi}F_+^{\rm SS2}\right] f_+^{a*} + i(A'+B')\left[\frac{nc}{2\pi}F_+^{\rm SS}B_-^{\rm SS}\right] b_-^{a*} , \tag{A23a}$$

$$\frac{db_-^S}{dz} = \left[\frac{\lambda}{c} + iK_\perp - i(A'+B')I_f + i2A'I_b\right] b_-^S - i(A'+B')\left[\frac{nc}{2\pi}F_+^{\rm SS*}B_-^{\rm SS}\right] f_+^S - i(A'+B')\left[\frac{nc}{2\pi}F_+^{\rm SS}B_+^{\rm SS}\right] f_+^{a*} - iA'\left[\frac{nc}{2\pi}B_-^{\rm SS2}\right] b_-^{a*} , \tag{A23b}$$

$$\frac{df_+^{a*}}{dz} = -\left[\frac{\lambda}{c} - iK_\perp + i2A'I_f + i(A'+B')I_b\right] f_+^{a*} - i(A'+B')\left[\frac{nc}{2\pi}F_+^{\rm SS*}B_-^{\rm SS}\right] b_-^{a*} - iA'\left[\frac{nc}{2\pi}F_+^{\rm SS*2}\right] f_+^S - i(A'+B')\left[\frac{nc}{2\pi}F_+^{\rm SS*}B_-^{\rm SS*}\right] b_-^S , \tag{A23c}$$

$$\frac{db_-^{a*}}{dz} = \left[\frac{\lambda}{c} - iK_\perp + i(A'+B')I_f + i2A'I_b\right] b_-^{a*} + i(A'+B')\left[\frac{nc}{2\pi}F_+^{\rm SS}B_-^{\rm SS*}\right] f_+^{a*} + i(A'+B')\left[\frac{nc}{2\pi}F_+^{\rm SS}B_+^{\rm SS}\right] f_+^S + iA'\left[\frac{nc}{2\pi}B_-^{\rm SS*2}\right] b_-^S \tag{A23d}$$

where $I_f = (nc/2\pi)|F_+^{\rm SS}(0)|^2$ and $I_b = (nc/2\pi)|B_-^{\rm SS}(L)|^2$ are the input intensities. The linearized equations for the four polarization-perturbating fields decouple into two sets of two equations which couple the forward- (backward-) going Stokes field with the backward- (forward-) going anti-Stokes field and which are given by

$$\frac{df_-^S}{dz}=\left[-\frac{\lambda}{c}-iK_\perp+i(A'+B')I_f+i2A'I_b\right]f_-^S+i(A'+B')\left[\frac{nc}{2\pi}F_+^{SS}B_-^{SS}\right]b_+^{a*}\,, \tag{A24a}$$

$$\frac{db_+^{a*}}{dz}=\left[\frac{\lambda}{c}-iK_\perp+i2A'I_f+i(A'+B')I_b\right]b_+^{a*}+i(A'+B')\left[\frac{nc}{2\pi}F_+^{SS*}B_-^{SS*}\right]f_-^S\,. \tag{A24b}$$

We make the following transformation:

$$f_j^i(z)=\tilde{f}_j^i(z)\exp\{i[A'I_f+(A'+B')I_b]z\}\,, \tag{A25a}$$

$$b_j^i(z)=\tilde{b}_j^i(z)\exp\{-i[(A'+B')I_f+A'I_b]z\} \tag{A25b}$$

where $i=S,a$ and $j=+,-$. Substitution of Eqs. (25) into Eqs. (24) yields the following equation for the amplitude-perturbation fields:

$$\frac{d}{dz/L}\begin{bmatrix}\tilde{f}_+^S\\ \tilde{b}_-^S\\ \tilde{f}_+^{a*}\\ \tilde{b}_-^{a*}\end{bmatrix}=\begin{bmatrix}-\lambda T_t-iK_\perp L+iP_f' & i(1+r)\sqrt{P_f'P_b'} & iP_f' & i(1+r)\sqrt{P_f'P_b'}\\ -i(1+r)\sqrt{P_f'P_b'} & \lambda T_t+iK_\perp L-iP_b' & -i(1+r)\sqrt{P_f'P_b'} & -iP_b'\\ -iP_f' & -i(1+r)\sqrt{P_f'P_b'} & -\lambda T_t+iK_\perp L-iP_f' & -i(1+r)\sqrt{P_f'P_b'}\\ i(1+r)\sqrt{P_f'P_b'} & iP_b' & i(1+r)\sqrt{P_f'P_b'} & \lambda T_t-iK_\perp L+iP_b'\end{bmatrix}\begin{bmatrix}\tilde{f}_+^S\\ \tilde{b}_-^S\\ \tilde{f}_+^{a*}\\ \tilde{b}_-^{a*}\end{bmatrix} \tag{A26}$$

and for the polarization-perturbation fields

$$\frac{d}{dz/L}\begin{bmatrix}\tilde{f}_-^S\\ \tilde{b}_+^{a*}\end{bmatrix}=\begin{bmatrix}-\lambda T_t-iK_\perp L+irP_f'+i(1-r)P_b' & i(1+r)\sqrt{P_f'P_b'}\\ i(1+r)\sqrt{P_f'P_b'} & \lambda T_t+iK_\perp L+i(1-r)P_f'+irP_b'\end{bmatrix}\begin{bmatrix}\tilde{f}_-^S\\ \tilde{b}_+^{a*}\end{bmatrix}. \tag{A27}$$

From these two sets of equations, we complete the stability analysis in a manner entirely analogous to that for the amplitude perturbation fields for the linear and parallel eigenpolarization.

---

*Present address: School of Applied and Engineering Physics, Cornell University, Ithaca, NY 14853.

[1] Y. Silberberg and I. Bar-Joseph, Phys. Rev. Lett. **48**, 1541 (1982).

[2] Y. Silberberg and I. Bar-Joseph, J. Opt. Soc. Am. B **1**, 662 (1984).

[3] I. Bar-Joseph and Y. Silberberg, Phys. Rev. A **36**, 1731 (1987); R. Chang and P. Meystre, *ibid.* **44**, 3188 (1991).

[4] G. Khitrova, J. F. Valley, and H. M. Gibbs, Phys. Rev. Lett. **60**, 1126 (1988).

[5] C. T. Law and A. E. Kaplan, J. Opt. Soc. Am. B **8**, 58 (1991).

[6] The subject of polarization instabilities has recently been reviewed by N. I. Zheludev, Usp. Fiz. Nauk **157**, 683 (1989) [Sov. Phys. Usp. **32**, 357 (1989)].

[7] D. M. Pepper, D. Fekete, and A. Yariv, Appl. Phys. Lett. **33**, 41 (1978).

[8] A. Yariv and D. M. Pepper, Opt. Lett. **1**, 16 (1977).

[9] H. G. Winful and J. H. Marburger, Appl. Phys. Lett. **36**, 613 (1980).

[10] R. Lytel, J. Opt. Soc. Am. B **1**, 91 (1984).

[11] A. E. Kaplan and C. T. Law, IEEE J. Quantum Electron. **21**, 1529 (1985).

[12] D. J. Gauthier, M. S. Malcuit, A. L. Gaeta, and R. W. Boyd, Phys. Rev. Lett. **64**, 1721 (1990).

[13] A. E. Kaplan, Opt. Lett. **8**, 560 (1983).

[14] S. Wabnitz and G. Gregori, Opt. Commun. **59**, 72 (1986).

[15] M. V. Tratnik and J. E. Sipe, Phys. Rev. A **35**, 2965 (1987); **35**, 2976 (1987); **36**, 4817 (1987).

[16] J. Yumoto and K. Otsuka, Phys. Rev. Lett. **54**, 1806 (1985).

[17] A. L. Gaeta, R. W. Boyd, J. R. Ackerhalt, and P. W. Milonni, Phys. Rev. Lett. **58**, 2432 (1987).

[18] D. J. Gauthier, M. S. Malcuit, and R. W. Boyd, Phys. Rev. Lett. **61**, 1827 (1988).

[19] S. N. Vlasov and V. I. Talanov, in *Optical Phase Conjugation in Nonlinear Media, V,* edited by I. Bespalov (Institute of Applied Physics, USSR Academy of Sciences, Gorki, 1979), pp. 85–91; B. Ya. Zel'dovich, N. F. Pilipetsky, and V. V. Shkunov, *Principles of Phase Conjugation* (Springer-Verlag, New York, 1985), pp. 165–167; W. J. Firth and C. Paré, Opt. Lett. **13**, 1096 (1988); G. Grynberg and J. Paye, Europhys. Lett. **8**, 29 (1989); G. G. Luther and C. J. McKinstrie, J. Opt. Soc. Am. B **7**, 1125 (1990); **9**, 1047 (1992).

[20] W. J. Firth, A. Fitzgerald, and C. Paré, J. Opt. Soc. Am. B **7**, (1990).

[21] N. Tan-No, T. Hashimiya, and H. Inabe, IEEE J. Quantum Electron. **16**, 147 (1980); J. Pender and L. Hesselink, Opt. Lett. **2**, 58 (1987); G. Grynberg, E. Le Bihan, P. Verkerk, P. Simoneau, J. R. R. Leite, D. Bloch, S. Le Boiteux, and M. Ducloy, Opt. Commun. **67**, 363 (1988).

[22] J. Pender and L. Hesselink, Opt. Lett. **12**, 693 (1987).

[23] G. Grynberg, E. LeBihan, P. Verkerk, P. Simoneau, J. R. R. Leite, D. Bloch, S. le Boiteux, and M. Ducloy, Opt. Commun. **67**, 363 (1988).

[24] A. Petrossian, M. Inard, A. Maitre, J.-Y. Courtois, and G. Grynberg, Europhys. Lett. **18**, 689 (1992).

[25] G. Grynberg, Opt. Commun. **66**, 321 (1988).
[26] R. Chang, W. J. Firth, R. Indik, J. V. Moloney, and E. M. Wright, Opt. Commun. **88**, 167 (1992).
[27] A. L. Gaeta and R. W. Boyd (unpublished).
[28] W. J. Firth and C. Penman, in *OSA Proceeding on Nonlinear Dynamics in Optical Systems,* edited by N. B. Abraham, E. Garmire, and P. Mandel (Optical Society of America, Washington, DC, 1991), Vol. 7, pp. 142–145.
[29] J. V. Moloney, M. R. Belic, and H. M. Gibbs, Opt. Commun. **41**, 397 (1982).